

## ELECTRON EMISSION AND DIFFRACTION BY A COPPER CRYSTAL\*

BY H. E. FARNSWORTH  
BROWN UNIVERSITY, PROVIDENCE, R. I.

(Received July 19, 1929)

## ABSTRACT

**Correlation between changes in slope of secondary electron curve, and position of diffraction beams.**—A narrow beam of electrons of variable speed is incident normally on the (100) face of a copper crystal. Measurements of the total secondary electron current are obtained under the same conditions as the angular distribution of scattered electrons for bombarding potentials from 0 to 250 volts, and after the crystal has been thoroughly degassed at red heat in an exceptionally good vacuum. The total secondary electron curve shows two maxima at 3 and 10.5 volts, respectively, and many sudden changes in slope in the region between 10.5 and 250 volts. Intense beams of full-speed electrons are found to issue from the crystal at such voltages as to account for the maxima, and for many of the changes in slope. Other beams are to be expected in the direction of the normal to the crystal, and hence are outside the solid angle of observation; they, however, contribute to the total secondary current, and appear sufficient to account for the remaining changes in slope. It thus appears that changes in the electron emission at potentials corresponding to energy levels within the atom are, at most, relatively unimportant in the production of sudden changes in slope in this region.

**Diffraction beams.**—With two exceptions, all of the expected diffraction beams which are the x-ray analogues in the two principal azimuths, and in the range below 250 volts are found. In addition, 20 sets of beams are found, 12 of which satisfy the conditions required by a wave of one-half the length given by  $\lambda = h/mv$ , or by a double grating spacing. These beams appear not to be due to gas. A temperature effect is observed for both types of beams. One additional set of beams at 3 volts does not appear in either of the two principal azimuths, and is not accurately reproducible. Most of the beams are very intense and sharp. In the case of a 70-volt beam, the background scattering of full-speed electrons in azimuth under the best vacuum conditions is found to be only 4.3 percent of the maximum intensity of the beam.

**Refractive index.**—Both types of classified beams require a refractive index greater than unity. The value of  $\phi$ , however, in the expression  $\mu = (1 + \phi/V)^{1/2}$  is not constant, but increases from 6 or 7 volts for beams at the lowest voltages to about 25 volts for the beams above 200 volts.

**Energy of scattered electrons.**—After making correction for an error inherent in the method of measurement, it appears that the diffraction beams are composed entirely of full-speed electrons. These electrons in the case of the 70 volt beam comprise about 50 percent of all the electrons moving in the direction of the beam. *Evidence of a selective angular distribution of emitted electrons*, differing from that of the scattered electrons, is also obtained.

**I**N A series of investigations<sup>1</sup> the writer has previously shown that the sudden changes in slope in the low-voltage region of the secondary electron curve

\* A preliminary account of some of the results reported here is given in *Nature* **123**, 941 (1929).

<sup>1</sup> H. E. Farnsworth, *Phys. Rev.* **25**, 41 (1925); **31**, 419 (1928).

(total secondary electron current as a function of bombarding potential) of polycrystalline copper are a function of the arrangement of the surface atoms, and not directly of the structure of the atoms themselves. Since the development of the idea of electron diffraction, it appears natural to attribute these results to the wave nature of the electron. Some evidence of this has already been furnished by experiments<sup>2</sup> in which a change was observed in the angular distribution of the secondary electrons concomitant with the appearance of the changes in slope, mentioned above, which resulted from critical heat-treatment of the target. It appeared advisable, however, to carry out a more direct experiment by measuring the total secondary emission from a single copper crystal under the same conditions as the angular distribution of scattered electrons, and thus make possible a correlation between the voltages corresponding to the changes in slope of the secondary electron curve and the voltages corresponding to the diffraction beams.

This was the original object of the experiments reported here. However, during the course of the experiments there have been certain developments which made it advisable to investigate, in addition, other points of importance. Among these is the subject of refractive index. The results of Davisson and Germer<sup>3</sup> for the (111) face of a nickel crystal require a refractive index in accord with the equation  $\mu = (1 + \phi/V)^{1/2}$  where  $V$  is the bombarding voltage, and  $\phi$  is the inner potential of the crystal which has the constant value of about 18 volts, except for a voltage range in which  $\mu$  appears anomalous. On the other hand, the results of Rose<sup>4</sup> for the (111) face of an aluminum crystal require a refractive index of unity. Although Rupp,<sup>5</sup> from a study of the transmission of slow electrons through thin metal films, has reported a refractive index greater than unity, G. P. Thomson<sup>6</sup> has shown that Rupp's reasoning was in error, and that his results furnish no information in regard to refractive index. The above experiments leave the subject of refractive index unsettled.

Results on certain other important points which have been investigated are also contained in this report.

#### APPARATUS AND PROCEDURE

The essential parts of the apparatus are shown diagrammatically in Fig. 1. They are constructed of molybdenum to eliminate magnetic effects. The earth's magnetic field is compensated by Helmholtz coils of 1 meter diameter. A special type of electron gun *SFAB* is used to obtain an intense beam of electrons at the low voltages. It is essentially the same as that previously described,<sup>7</sup> except for the construction of the part *B*. In the present case the construction is such as to permit the maximum possible motion of the

<sup>2</sup> H. E. Farnsworth, Phys. Rev. **31**, 414 (1928).

<sup>3</sup> Davisson and Germer, Phys. Rev. **30**, 705 (1927); Proc. Nat. Acad. Sc. **14**, 619 (1928).

<sup>4</sup> D. C. Rose, Phil. Mag. **6**, 712 (1928).

<sup>5</sup> E. Rupp, Ann. d. Physik **85**, 981 (1928).

<sup>6</sup> G. P. Thomson, Phil. Mag. **6**, 939 (1928).

<sup>7</sup> H. E. Farnsworth, J.O.S.A. and R.S.I. **15**, 290 (1927).

Faraday box *G*. In addition, a ring is attached to *B* which covers the space between *A* and *B*, and thus prevents stray electrons from leaving at this place. The primary electrons strike, at normal incidence, the (100) face of the copper crystal *T* which is placed at the center of the drum *C*. One edge of the drum is made with a slot so that some electrons, after leaving the crystal, may pass through it, and into the opening of the double Faraday box which may be rotated in a horizontal plane from the plane of the target to within  $13^\circ$  of the incident beam. The double box is made with a rectangular cross-section. The sides of each box are made in one piece, properly folded; the ends have projecting pieces which fit snugly over the sides, and hold them in place. The two boxes are insulated from each other by quartz strips. The whole arrangement is assembled with cleaned metal tweezers so that all parts of the box are free from contamination. A fine platinum wire which makes contact with the inner box is shielded by quartz tubing, and passes outward

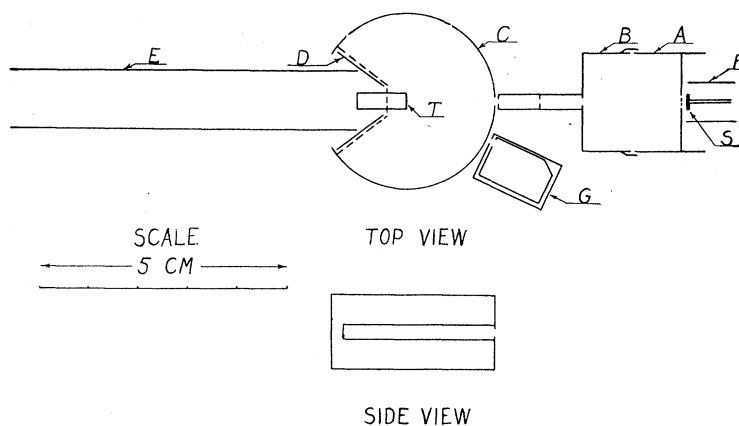


Fig. 1. Apparatus.

from the drum along the axis of revolution. During observations on angular distribution the potential of the inside Faraday box is so adjusted that electrons which have lost more than one volt at the crystal are excluded from the box.

The crystal is mounted on a quartz strip which is rigidly attached to the end of a Pyrex tube by means of a tungsten rod sealed into the end of the tube. The axis of the tube is perpendicular to the face of the crystal. This tube may be rotated or slid in guides parallel to its axis, thus rotating the crystal in azimuth, or removing it into a side tube where it may be heated at red heat. A molybdenum strip, making good thermal contact with the back of the crystal, is heated by electron bombardment, and the crystal is thus heated by conduction. This method of heating was found to decrease the amount of recrystallization which occurred at the place of bombardment of the copper crystal. The crystal was heated so that copper evaporated freely from the surface. A trap-door may be raised in the side tube, after

withdrawing the crystal, to prevent copper vapor from entering the apparatus proper, and thus contaminating insulating surfaces.

The moving parts are operated by two magnetic controls which are sufficiently far removed (from 10 to 12 inches) to cause no measurable effect at the target. The bearings are molybdenum on molybdenum and molybdenum on Pyrex glass.

The metal parts are enclosed in a Pyrex tube in the form of a 3 inch bulb with properly arranged side tubes. The inside of the bulb was made conducting by evaporation from a molybdenum filament. The coating is sufficiently thin to permit observation through it when properly illuminated. This serves as an electrostatic shield, and also permits a measure of the electrons which escape through the slot in the drum. The various metal parts, with the exception of the cylinder *E* and the target *T*, are mounted on a Pyrex framework. *E* and *T* are mounted on another framework. These two frames were inserted in opposite side tubes, and were brought together in proper alignment by guides attached to the frames. When in place, the crystal is at the center of the bulb.

The total primary current is obtained by measuring the current to the cylinder *E* and crystal, with the crystal withdrawn to the back end; or by measuring the total current to target, shield, drum and diaphragm *D*, with the target in the forward position. Since both methods give the same result, the latter is used in practice. The total secondary current is then obtained in the usual manner by subtracting the current to the target from the total current. With the crystal withdrawn, no current is observed to the drum *C* or diaphragm *D*, thus insuring that the primary beam is not scattered.

The total primary and secondary currents are measured with a galvanometer of sensitivity  $10^{-9}$  amperes per mm on a scale at 1 m distant. The current to the Faraday box is measured by a Compton electrometer of sensitivity about 1000 mm per volt shunted with India ink resistances so as to give a current sensitivity of approximately  $10^{-12}$  amperes per mm on a scale at 1 m distant.

All metal and glass parts of the tube were thoroughly cleaned with chromic acid and distilled water either before or after mounting in place. Where mounting was necessary after cleaning, the parts came in contact with only cleaned rubber gloves or metal tweezers. The tube was baked and pumped for several days.

The pumping system consists of two Pyrex diffusion-pumps and an oil-pump, in series. The mercury shut-off is placed between the two diffusion-pumps so that the minimum length of large glass tubing, which includes a mercury-vapor trap in liquid air, separates the experimental tube from the first diffusion-pump. The diffusion-pumps are kept running during observations. It was originally intended to seal the tube from the pumping system, but the vacuum conditions obtained are sufficiently good without. Under the best conditions no pressure is observable on a sensitive McLeod gauge (a distance of 0.75 mm in the top of the gauge capillary corresponds to  $10^{-6}$  mm Hg) while the crystal is at red heat. Also, the tube has remained as long as

48 hours after stopping the pumps with no pressure observable on the gauge at the end of this time. The good vacuum conditions are attributed, in part, to an additional condensing trap in liquid air which is placed between the oil-fore-pump and the diffusion-pumps, thus preventing any oil vapor from contaminating the mercury in the pumps, and from entering the other liquid-air trap.\* This second trap is made of small tubing, and is placed beside the large trap so that one liquid-air container serves to cool both traps.

The crystal was heated separately at red heat for several minutes after baking the whole tube so as to remove the layer of oxide on the crystal face. A series of observations, extending over a period of several weeks, was then made to locate diffraction beams in the two principal azimuths, and in the voltage range from 0 to 150 volts. This consisted in taking colatitude curves for various bombarding potentials so that the complete range was covered in steps of a few volts, and also in obtaining several azimuth curves for the beams. During this period the crystal was not heated; it was probably not well degassed since the total time of heating had been rather short. The time of heating the crystal was purposely made short since two other copper crystals had been damaged by heat-treatment. After the above procedure the crystal was further heated at red heat until it was thoroughly degassed, and the same complete range again investigated. Since the intensity of the electron beams decreased gradually with time, the procedure was adopted of heating the target at red heat each day for about one minute, one-half hour previous to beginning observations. Results were obtained below 150 volts in at least two opposite angles of each azimuth, and over parts of the range in all four angles of each azimuth. The observations were later extended to 250 volts in one of each of the two principal azimuths.

#### PREPARATION AND GEOMETRY OF THE CRYSTAL

The copper crystal was obtained from the General Electric Co. It was made by melting and slow cooling in an atmosphere of hydrogen. The approximate orientation of the crystal was determined by a method described by Bridgman.<sup>8</sup> Etching in ammonium persulphate develops both the (100) and (111) faces. A piece of the crystal to be used for the target was carefully cut, with a jeweler's saw, so that one geometrical face was as nearly parallel as possible to a (100) plane. To make the face more nearly parallel to this plane, the following method was used. The crystal was mounted in a wooden holder on the tool-post of a lathe so that the crystal plane in question was approximately perpendicular to the axis of the lathe. After reflection from a small mirror, a narrow beam of light was sent along the axis of the lathe, and reflected by the crystal back to a telescope placed just behind and to one side of the mirror. The adjustment consisted in changing the orientation of the crystal until the crystal facets flashed out in the field of the telescope. The crystal plane in question was then perpendicular to the axis of the lathe. A fine grinding wheel was then mounted on the lathe

\* This idea developed during a conversation with Mr. Theodore Soller.

<sup>8</sup> P. W. Bridgman, Proc. Am. Acad. Sc. **60**, 313 (1925).

so that it rotated about an axis parallel to the axis of the lathe. Without changing its orientation, the crystal was brought into contact with the grinding wheel which was slowly rotated until a flat surface was produced on the crystal. By re-etching the surface and repeating the above process a few times the desired result was obtained to sufficient accuracy.

After the target has been cut and surfaced it is essential that it be etched sufficiently to remove all broken pieces from the surface. Unless this is done these small crystals will grow at the expense of the larger crystal during subsequent heating.

Since the copper crystal is a face-centered cube, it follows that for normal incidence on the (100) plane there exist four-fold symmetry and two principal azimuths. The azimuths parallel to the cube sides will be denoted as the (100) azimuths, and those parallel to the face-diagonals as the (111) azimuths, in accord with Fig. 2a. When viewed from a direction perpendicular to a (100) plane, the rows of atoms perpendicular to this plane intersect it in points which are represented by circles and crosses in Fig. 2b. If the circles

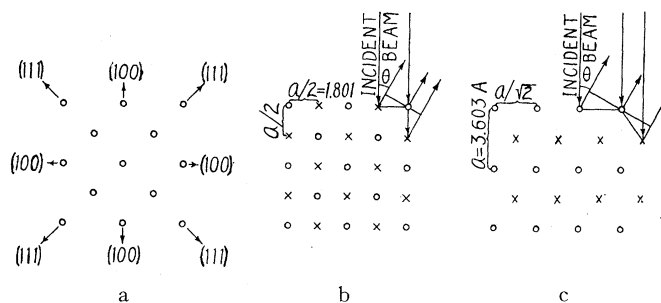


Fig. 2 Structure of the crystal. a—The (100) face and azimuth designation. b—The (100) azimuth. c—The (111) azimuth.

denote atoms lying in the plane of the paper, then the crosses represent atoms lying in front or in back of this plane by an amount  $a/2 = 1.801\text{A}$ . When viewed from a direction perpendicular to a (110) plane, the rows of atoms perpendicular to this face intersect it in points which are shown in Fig. 2c. If the circles represent atoms lying in the plane of the paper, then the crosses represent atoms lying in front or in back of this plane by an amount  $a/2(2)^{1/2} = 1.275$ . The azimuths lying in or parallel to the plane of the paper are then the (100) and (111) azimuths for Figs. 2 b and 2c, respectively. The (111) azimuth is also the (110) azimuth.

The positions of the theoretical or Laue beams were determined by applying the conditions for constructive interference to radiation coming from rows or lines of atoms perpendicular to the azimuths in question.

Referring to Fig. 2b for the (100) azimuth, the radiation is incident on the crystal in the vertical direction. Let the direction making an angle  $\theta$  with the vertical, as shown by the arrows, be one in which there is constructive interference. It is seen that if the conditions of constructive interference are satisfied by the three rows of atoms considered, then they will also be satisfied

by all other rows of atoms. These conditions may be stated in the form of the two equations

$$n_1\lambda = 1.8015 \sin \theta, \quad n_2\lambda = 1.8015(1 + \cos \theta),$$

where  $n_1$  and  $n_2$  may have any integer values. Solving these two equations simultaneously, one obtains the corresponding values of  $\lambda$  and  $\theta$  for various values of  $n_1$  and  $n_2$ . The graphical method is given here since it offers a simple method of designating the orders to which the various points correspond. The plots of  $\lambda$  against  $\sin \theta$  obtained from the above equations for various

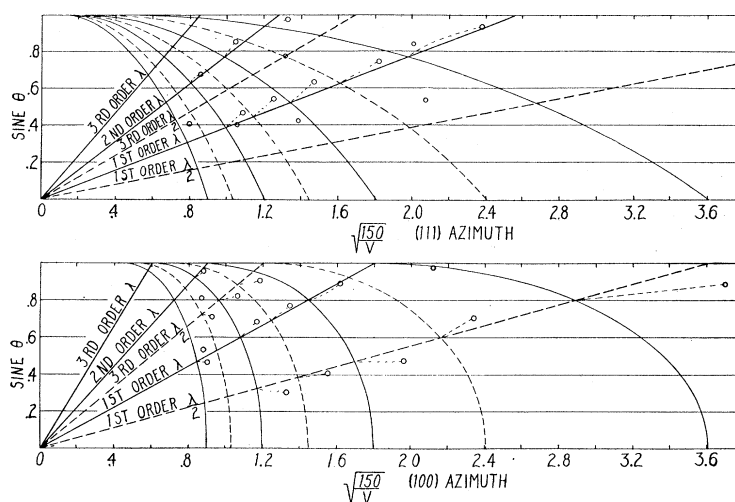


Fig. 3. Location of experimental and theoretical diffraction beams on a plot of  $\sin \theta$  against  $\lambda = (150/V)^{1/2}$ . Positions of experimental beams are denoted by circles and of theoretical  $\lambda$ -beams by the intersections of continuous curves. Intersections of broken lines with either broken or continuous lines denote the positions of theoretical  $\lambda/2$ -beams.

values of  $n_1$  and  $n_2$  are shown by the continuous lines in Fig. 3. The positions of the theoretical beams are then given by the intersections of these lines. Referring to Fig. 2c, by a similar consideration for the (111) azimuth, the following two equations are obtained:

$$n_1\lambda = 2.55 \sin \theta, \quad n_2\lambda = 1.8015 + 2.2070 \cos (\theta + 35^\circ 15.6').$$

The plots of  $\lambda$  against  $\sin \theta$  obtained from these two equations are also shown by continuous lines in Fig. 3. These lines determine the positions of the theoretical beams in the (111) azimuth by their points of intersection.

The angular positions and voltages of the diffraction beams occurring in the (100) and (111) azimuths and in the region from 0 to 250 volts are shown in Table I and in the plot of Fig. 3. The theoretical voltages in column 2 of Table I are obtained from the expression  $V = 150/\lambda^2$ , where  $\lambda$  is the wavelength of the theoretical beams taken from Fig. 3. The voltage differences give the values of  $\phi$  which appear in the expression  $\mu = (1 + \phi/V)^{1/2}$  for refractive

TABLE I. *Diffraction Beams.*

Experimental voltage of electron beam	Theoretical voltage for $\mu = 1, V = 150/\lambda^2$	Voltage difference	Colatitude angle
(100) Azimuth			
57.2	72.3	15.1	63.0°
110.0	129.0	19.0	43.5°
186.5	212.2	25.7	27.5°
196.5	218.0	21.5	72.5°
"Additional Beams"			
11.0	18.1	7.1	62.5°
27.5	32.4	5.9	45.0°
33.5	—	—	78.0°
39.0	52.5	13.5	28.0°
62.5	77.6	15.1	24.0°
82.5	96.8	14.3	50.0°
85.0	109.0	24.0	17.5°
107.5	133.6	26.1	65.0°
132.5	162.7	30.2	56.0°
176.5	198.0	21.5	45.0°
194.0	—	—	32.0°
199.0	—	—	54.0°
(111) Azimuth			
26.5	38.8	12.3	70.0°
70.0	84.0	14.0	39.3°
85.0	105.1	20.1	77.0°
128.0	153.5	25.5	27.8°
135.5	155.8	20.3	56.5°
206.5	234.0	27.5	42.5°
—	245.0	—	—
—	266.0	—	—
"Additional Beams"			
35.0	—	—	32.5°
37.5	—	—	57.0°
45.5	58.5	13.0	48.0°
79.0	—	—	25.0°
87.5	87.5	0	50.8°
96.0	115.3	19.3	32.7°
137.0	—	—	23.5°
236.5	—	—	24.0°

index. In addition to the beams for which there are x-ray analogues, several others are observed which have been tabulated under "additional beams." Many of these beams occupy the approximate positions which would be expected for a wave of one-half the length given by the expression  $\lambda = h/mv$  or for a space grating of twice the spacing for a copper crystal. For convenience of notation such beams will be referred to as  $\lambda/2$ -beams. Positions of the theoretical beams to which these  $\lambda/2$ -beams correspond are given by the intersections of broken lines with either broken or continuous lines. The broken lines are obtained from the same equations that give the continuous lines, except that  $\lambda$  is replaced by  $\lambda/2$ . Hence, the continuous lines of any particular order coincide with broken lines of twice the order. Davisson and Germer<sup>9</sup> have also observed beams which satisfy the same relation, but which are plane grating beams instead of space grating beams. These beams dis-

<sup>9</sup> Davisson and Germer, Phys. Rev. **30**, 705 (1927); L. H. Germer, Zeits. f. Physik **54**, 408 (1929).



appeared with further heating of the nickel crystal, and hence were attributed to a surface gas grating having twice the spacing of the nickel grating.

The "additional beams" which are observed for the copper crystal do not appear to be due to gas for the following reasons: (1) They are space grating beams instead of surface grating beams, i.e., they are sharp in colatitude angle as well as voltage, and of the same order of intensity as other beams. (2) They are observed under the best vacuum conditions which must be of the order of  $10^{-8}$  mm Hg, and show no indication of decreasing in intensity with further heating of the crystal. (3) They are observed only a few minutes after the crystal has been heated at red heat, i.e., while it is still considerably above room temperature, and exhibit a temperature effect similar to that of the other beams. They attain their maximum intensity about one-half hour after heating, which then decreases very slowly (see Temperature Effect below). (4) Three sets of the "additional beams" fall on first order lines i.e., they are not "half order" beams. They appear too intense to be attributed to a second order beam from a double spaced surface grating. (5) Two sets of beams not satisfying the relation of the majority of the "additional beams" were found to disappear with further heating of the crystal. These may have been due to gas or a trace of copper oxide on the surface.

As mentioned above, these results appear to require an additional wavelength or an additional grating spacing. In either case, the absence of many "additional beams" which are required to satisfy all of the  $\lambda/2$ -relations is unaccounted for. If the results are attributed to the grating it must be a volume effect, as pointed out above. The type of beams in (4) above would then require the constructive interference of radiation from a surface grating of single spacing with that from a depth grating of double spacing. The fact that most of these beams appear in the (100) azimuth makes it seem that the structure of the crystal is responsible for them.

The following is a summary of the electron beams found to issue from the crystal in the two principal azimuths and in the region 0 to 250 volts:

Ten sets of electron beams are found which are the x-ray analogues, and which require a refractive index greater than unity. This includes three 1st order and three 2nd order sets of beams in the (111) azimuth; three 1st order and one 2nd order sets of beams in the (100) azimuth. One 3rd order and one 1st order set in the (111) azimuth which should appear in this voltage range are missing. In addition, 12 sets of beams appear in the (100) azimuth, 8 of which satisfy the  $\lambda/2$ -relation, and require a refractive index greater than unity. Three of the remaining beams are very weak. The fourth is quite strong, and falls near one of the x-ray beams which is associated with another electron beam. In the (111) azimuth, three sets are accounted for by the  $\lambda/2$ -relation, one of which requires a refractive index of unity. There are 4 other sets in this azimuth, all of which are very weak. Besides the above, the observed set of 3 volt beams does not appear in either azimuth, and is not accurately reproducible.

Some of the typical beams are shown in both colatitude and azimuth in Figs. 4, 5, and 6. It is to be noted that the beam in Fig. 6 is an "additional beam" to which statement (4) above applies. The effect of heating the crystal

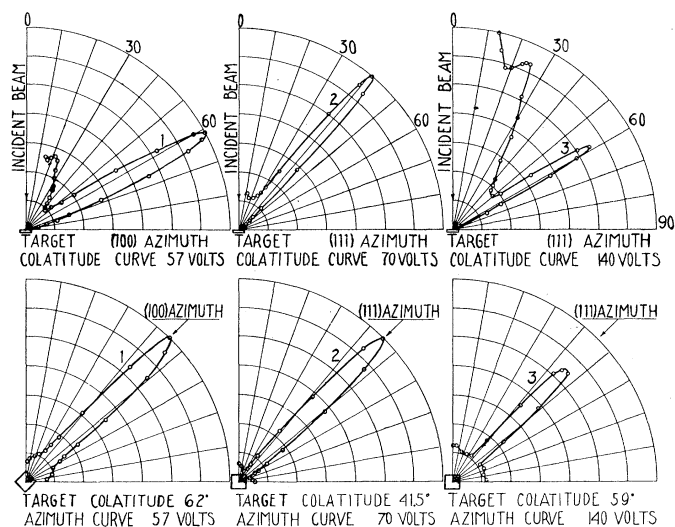


Fig. 4. Beams 1 and 2 are 1st order  $\lambda$ -beams. Beam 3 is a 2nd order  $\lambda$ -beam.

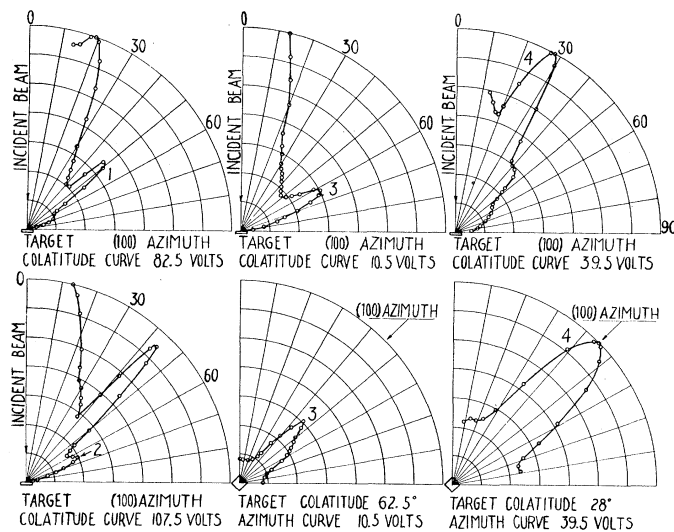


Fig. 5. Beam 1 is a  $\lambda/2$ -beam on the 1st order  $\lambda$ -line. Beam 2 is a 3rd order  $\lambda/2$ -beam. Beams 3 and 4 are 1st order  $\lambda/2$ -beams.

has been to increase the intensity and sharpness of the beams. Some weak beams, which were not found after the initial heating, appeared after subsequent heating. No correction has been made to the colatitude angles to

take into account the effect of background scattering since it is small for most of the beams.

A variation in the colatitude angles for the different beams of a single set indicates that the normal to the crystal face makes an angle of about  $2.5^\circ$  with the incident beam in the plane of a (100) azimuth. The positions of the beams in Fig. 3 and Table I have been corrected for this imperfect alignment. The lack of exact symmetry in azimuth, as shown in Fig. 6, is attributed to this tilt of the crystal face. This lack of symmetry varies in amount with the colatitude angle of the beam, and hence produces an observed variation in azimuth for beams of different colatitude angles.

No attempt has so far been made to make an accurate comparison of intensities of the different beams. Such a comparison would require a knowledge of the actual values of total primary current as well as the values of

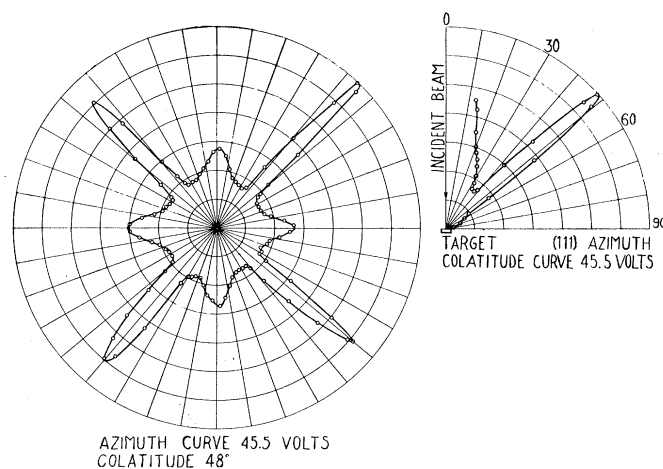


Fig. 6. A  $\lambda/2$ -beam showing symmetry in azimuth, and position in colatitude.

the corresponding currents to the Faraday box, since the total primary current cannot be held constant for all of the beams. In addition, a correction would be necessary for background scattering which differs for each beam.

The values of the voltage difference  $\phi$  given in column 3 of Table I are plotted against the theoretical voltage in Fig. 7. This curve shows that the voltage difference  $\phi$ , instead of being constant, decreases for the lower bombarding potentials, and approaches a limiting value for the higher potentials. This statement also applies to the "additional beams." It is believed that the deviation of the individual values from a smooth variation may well be due to various errors involved. It is impossible to determine the voltage for maximum development of some of the beams with a possible error of less than a few volts. The growth or decay of neighboring beams may falsify the voltage as well as the angular position of any one beam. In my note to "Nature," 30 volts was given for the upper value of  $\phi$ . Although one of the beams does appear to require this value, later observations at higher potentials indicate that 25 volts is more nearly the average for this upper value.

Davisson and Germer<sup>10</sup> found  $\phi$  for nickel to have the constant value of 18 volts, but their observations include only two beams below 100 volts at 54 and 65 volts, respectively. Davis<sup>11</sup> has recently found that a value of 4 or 5 volts for  $\phi$  is required in correlating maxima in the low voltage region of the secondary electron curve of polycrystalline cobalt with bands computed by the application of the Bragg formula to important sets of cobalt planes. From Fig. 7 it appears that the full value of this inner potential  $\phi$  of the crystal is not effective unless the incident electron speed exceeds a certain value. This suggests that  $\phi$  depends on the depth of penetration of the surface layer.

In making observations on total secondary electron emission from a metal target, it is found that after the target has been heated at red heat the apparent reflection coefficient passes through a minimum at a bombarding potential of about one volt, and then rapidly increases as the voltage is further decreased. In the past this has been attributed to a contact potential between the degassed target and the surrounding metal electrodes. Thus, if the target assumes a negative potential of one volt with respect to its

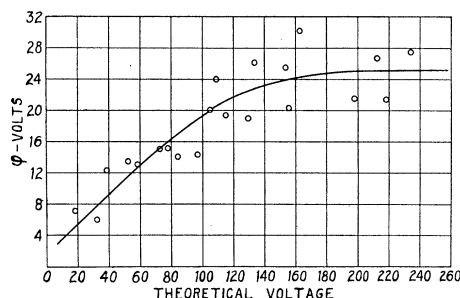


Fig. 7. Inner potential  $\phi$  of the crystal as a function of theoretical voltage of electron beams.

surroundings as a result of heat-treatment, then all primary electrons having an energy less than one equivalent volt are turned back from the target, and consequently increase the apparent reflection coefficient. To compensate for this effect the target has been placed at a positive potential of the correct amount. This is one volt for the copper crystal in the present experiments. However, recent theoretical investigations by Nordheim,<sup>12</sup> in terms of the new quantum mechanics, make it appear that an appreciable reflection coefficient is to be expected for very low-speed electrons. If this result is found to be in accord with experiment, then the effect observed is the combined effect of a contact potential difference and of a reflection coefficient. The present experimental arrangement affords no means of distinguishing between the two possibilities. In case the reflection coefficient proves to be responsible for an appreciable part of the effect, a correction must be applied to all experimental voltages in this paper. The effect of this correction would

<sup>10</sup> Davisson and Germer, Proc. Nat. Acad. Sc. **14**, 619 (1928).

<sup>11</sup> Myrl N. Davis, Nature **123**, 680 (1929).

<sup>12</sup> L. Nordheim, Zeits. f. Physik **46**, 833 (1928); Proc. Roy. Soc. **121**, 626 (1928).

be to decrease the values of  $\phi$ , given in column 3 of Table I, by an amount not greater than one volt.

An experiment is now being planned by the writer by which it is hoped that a distinction may be made between the above possibilities, and the effect of each separately determined.

#### TOTAL EMISSION

A comparison of the total secondary electron curve for the (100) face of a single copper crystal, as shown in Fig. 8, with that previously obtained for a polycrystalline copper surface<sup>1</sup> shows the presence of many more sudden changes in slope in the curve for the single crystal, although both curves show maxima and minima in the low-voltage region. It is also to be noted that the positions of the sudden changes in slope of the curve for

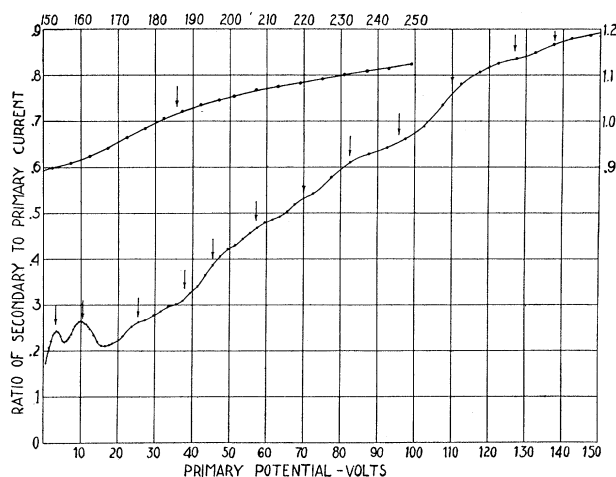


Fig. 8. Total secondary electron curve for the (100) face of a copper crystal. The upper curve is a continuation of the lower curve, and is plotted to the scales at the upper and right sides.

the single crystal do not coincide in voltage with any of those of the curve for the polycrystalline surface. These results confirm the statements in the first paragraph of this article. The arrows indicate the voltages at which intense diffraction beams are found to leave the crystal. They are such as to account for the two maxima and for many other changes in slope. Other beams are to be expected in the direction of the normal, and hence are outside the solid angle of observation; they, however, contribute to the total secondary current. For a refractive index of unity these beams in the region 0 to 250 volts would occur at 11.6, 46.3, 104.2, and 185 volts. Taking into account the actual refractive index, from Fig. 7, these beams should occur at approximately 7.5, 36, 84, and 160 volts. Similarly, there may be "additional beams" satisfying the  $\lambda/2$ -relation, for which the theoretical voltages are 26.0, 72.4, and 141.5 volts. When the values of refractive index are taken into account, these voltages should have the approximate values of

19, 57, and 118 volts. Although these values are only very approximate, a comparison with Fig. 8 shows that they are in satisfactory agreement with the curve, and appear to account for the changes in slope not accounted for by the observed beams.

The sharpness of the changes in slope of the curve is decreased by the fact that each electron beam is present over a range of several volts. This sharpness is still further decreased by the tilt of the target, which causes the voltages for the maximum development of the four beams in the four different angles of the same azimuth to have different values. When these factors are taken into account, it appears that most, if not all, of the departures from a smooth curve may be accounted for by the diffraction beams. In the low-voltage region, where the emission is negligible, these beams produce actual maxima in the curve. At higher voltages maxima do not occur because of the rapid increase in the number of emitted electrons with increase in voltage.

#### TEMPERATURE EFFECT

Davisson and Germer<sup>9</sup> have reported the effect of temperature of the nickel crystal on the intensity of the diffraction beams. A similar effect is observed in the present experiments for a copper crystal. The purpose of the curves in Fig. 9 is to verify the statement, previously made, that the "additional beams" show a temperature effect similar to that of the beams having x-ray analogues. The curves shown were obtained within five minutes after heating the target at red heat; hence the target was several hundred

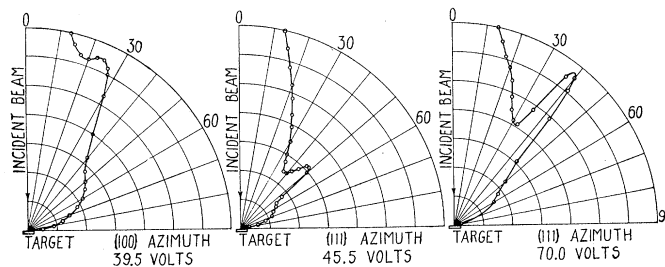


Fig. 9. The effect of increase in temperature of crystal on the relative strength of electron beams.

degrees C above room temperature during the observations. All of the beams investigated were found to be very weak in comparison with their relative intensity at room temperature, as shown in Figs. 4, 5, and 6. The intensity of the beams increases rapidly as the target cools; it attains a maximum value in about one-half hour, after which it decreases very gradually (only a few percent over a period of several hours).

#### RESOLVING POWER OF CRYSTAL AND APPARATUS

In general, the voltage range over which an electron beam is observable depends on the intensity of the beam and the value of the bombarding

potential. For example, the 26.5 volt beam can just be detected at 23.5 and at 30.5 volts. This gives a ratio of the observed range, expressed in wavelength difference, to the wavelength of the beam at maximum development of  $\Delta\lambda/\lambda = .125$ . The corresponding values for the 70.0 volt beam are 52.5 to 77.5 volts and  $\Delta\lambda/\lambda = .205$ ; for the 135.5 volt beam they are 125.5 to 145.5 volts, and  $\Delta\lambda/\lambda = .072$ .

The beams at the lower voltages move toward smaller colatitude angles as the voltage is increased, such that  $V^{1/2} \sin \theta$  remains approximately constant, but the beams at higher voltages grow and decay in a total angular displacement which is much smaller than the above relation requires. In fact, in some cases the position of the beam remains very nearly the same. Davisson and Germer attribute this failure to obey the plane grating formula to the lack of sufficiently wide crystal lattices.

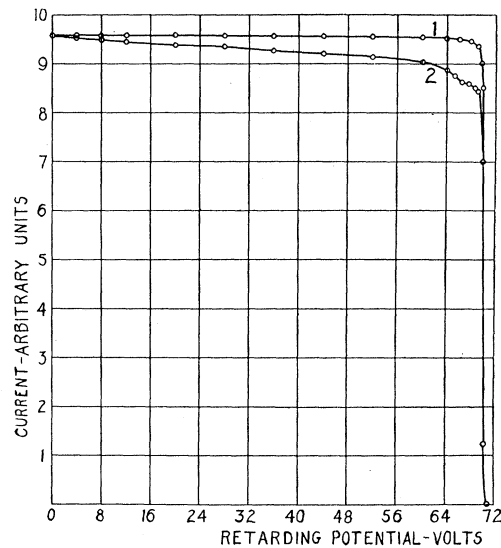


Fig. 10. Curve 1 shows correct energy distribution of primary electrons. Curve 2 shows apparent energy distribution of primary electrons.

The ratio of the background scattering to the maximum intensity of the diffraction beams is, in general, much smaller than the ratio observed by Davisson and Germer for a nickel crystal. This ratio for the 70 volt beam was found to be only 4.3 percent in azimuth under the best vacuum conditions. The beams for copper are also generally sharper in colatitude and azimuth than those for nickel, although some of the "additional beams" lack this extreme sharpness. Only a part of this difference for the two metals may be attributed to the difference in resolving power of the two pieces of apparatus.

The resolving power of the apparatus, as determined by the size of the opening in the Faraday box and its distance from the target (a 1 mm opening at 19 mm from the target), is less than the effective resolving power under

the conditions of observation. This results because the effective opening of the outer Faraday box is decreased by the retarding potential difference which exists between the boxes, i.e., only those high-speed electrons which are directed at a circular area somewhat smaller than the actual area of the opening, and concentric with it, are able to enter the inner box. That this is the case is shown by measurements with a similar arrangement on the primary beam whose correct energy distribution is known. The arrangement used for measurements on the primary beam is shown in Fig. 1. The primary beam passes through a 1 mm opening in the last diaphragm of the cylinder *B*, and then through an adjacent concentric opening of 2 mm diameter in the drum. By applying a retarding potential to the drum *C* and the electrodes *D* and *E* behind it, the shape of the field at the entrance of the drum should very closely approximate that at the entrance of the inner Faraday box, for the same potential differences. Curve 2, Fig. 10, shows the results of measurements of current to *C*, *D*, *T*, and *E* for various retarding potentials, and with a fixed primary voltage. The ratio of the difference between the ordinates of the two curves to the ordinate of the correct curve, at any particular retarding potential, should give the effective decrease in area for that retarding potential and for the primary potential used. This assumes, of course, a uniform distribution of current density over the area previous to the application of the retarding potential.

#### ENERGY DISTRIBUTION OF SCATTERED ELECTRONS

Referring again to Fig. 10, the energy distribution of the primary electrons, as expressed by curve 2, shows the presence of the main group of full-speed electrons and, in addition, a smaller group of nearly full-speed electrons. From the considerations contained in the previous paragraph, it follows that this second group is only apparent, and is caused by the geometry of the arrangement used for the measurements. Measurements on the energy distribution of scattered electrons by the method in question are hence subject to the same error, and require a correction. This correction may be approximately obtained from a comparison of the apparent and correct energy distributions of the primary beam. The correction may then be applied to the apparent energy distribution of the scattered electrons to obtain the correct energy distribution. This method of correction assumes the same distribution of current density across the primary and scattered beams that are being measured. Although this requirement is not fulfilled, at least an approximate correction can be made.

Taking the case of the 70 volt diffraction beam, curve 1 of Fig. 11 shows the current to the inner Faraday box as a function of the retarding potential between the two boxes. This curve represents the apparent distribution due to the sum of the emitted electrons, the background scattering, and the diffraction beam itself. The effects of the first two are eliminated by subtracting curve 2 which represents the apparent distribution of the emission and background scattering for the same voltage and colatitude angle, but different azimuth. Although the background scattering varies somewhat



with azimuth, the shape of the curve should not be very different. Similar estimates of the background scattering were also obtained by keeping the azimuth and colatitude angles unchanged, and varying the voltage. A curve obtained by the former method is shown here because it furnishes unexpected information regarding the emission. Comparison of curves 1 and 2 in the low-voltage region shows that there are more low-speed electrons in the azimuth-angle which does not contain the diffraction beam. Since the low-speed electrons are interpreted as emitted electrons, it follows that the emission is considerably greater in the azimuth-angle not containing the diffraction beam, and hence there is an angular distribution of emitted electrons which does not coincide with the angular distribution of scattered

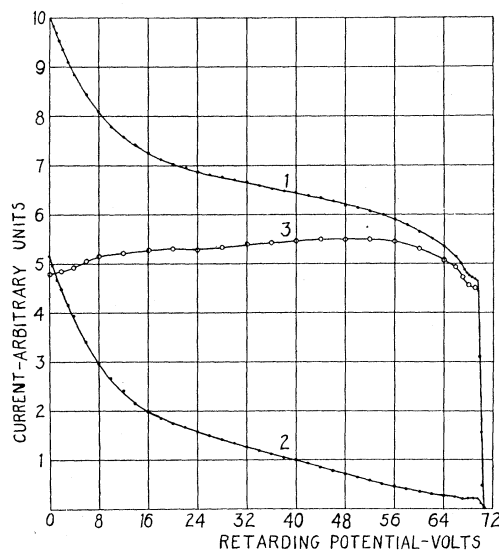


Fig. 11. Curve 1 shows apparent energy distribution of electrons in the 70 volt beam. Curve 2 shows apparent energy distribution of electrons for the same voltage and colatitude angle, but for azimuth angle differing by  $22.5^\circ$ . Curve 3 is obtained by subtracting curve 2 from curve 1.

electrons. This point has not been investigated in detail. The negative slope of curve 3 in the low-voltage region is, of course, a result of the distribution just mentioned. Returning now to a consideration of the scattered electrons, we see that, in addition to a group of full-speed electrons, there is an apparent group of nearly full-speed electrons similar to that shown in curve 2 of Fig. 10 for the primary beam. From the close similarity of these two curves it appears that this group of nearly full-speed electrons is entirely due to the defect in the method of measurement. Taking this, the background scattering, and the emission into account, it may be concluded that all of the electrons contributing to the diffraction beam considered are full-speed electrons.

Figure 12 shows two uncorrected energy distribution curves both of which are taken at the positions of the maximum development of diffraction beams.

A similar distribution is observed in these cases, although a smaller percent of full-speed electrons is present. In the case of the 70 volt beam the remarkable result is observed that at least 50 percent of all the electrons moving in the direction of the beam are full-speed electrons.

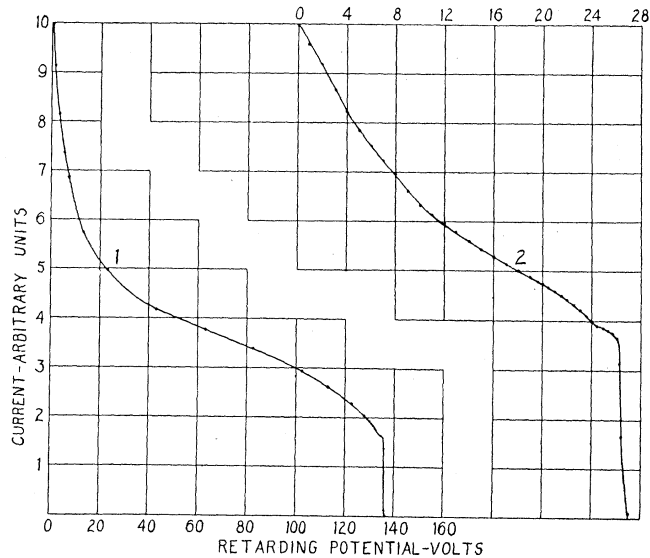


Fig. 12. Curve 1 shows apparent energy distribution of electrons in the 136 volt beam.  
Curve 2 shows apparent energy distribution of electrons in the 26.5 volt beam.

I have been greatly aided in these experiments by my research assistant, Mr. Newton Underwood. Most of the reducing and plotting of data has been done by Mr. Vernon Goerke. It is a pleasure to record here my sincere thanks to several Providence friends who have made this assistance possible. I am also indebted to the General Electric Co. for furnishing the copper crystal from which the target was cut.